

Provided for non-commercial research and education use.  
Not for reproduction, distribution or commercial use.



This article appeared in a journal published by Elsevier. The attached copy is furnished to the author for internal non-commercial research and education use, including for instruction at the authors institution and sharing with colleagues.

Other uses, including reproduction and distribution, or selling or licensing copies, or posting to personal, institutional or third party websites are prohibited.

In most cases authors are permitted to post their version of the article (e.g. in Word or Tex form) to their personal website or institutional repository. Authors requiring further information regarding Elsevier's archiving and manuscript policies are encouraged to visit:

<http://www.elsevier.com/copyright>



Contents lists available at ScienceDirect

## Journal of Non-Crystalline Solids

journal homepage: [www.elsevier.com/locate/jnoncrsol](http://www.elsevier.com/locate/jnoncrsol)

## High mixing entropy bulk metallic glasses

X.Q. Gao, K. Zhao, H.B. Ke, D.W. Ding, W.H. Wang, H.Y. Bai\*

Institute of Physics, Chinese Academy of Sciences, Beijing 100190, People's Republic of China

## ARTICLE INFO

## Article history:

Received 8 June 2011

Received in revised form 12 July 2011

Available online 4 August 2011

## Keywords:

High mixing entropy;

Bulk metallic glass;

Glass forming ability;

Mechanic property

## ABSTRACT

Bulk metallic glasses (BMGs) are usually based on a single principal element such as Zr, Cu, Mg and Fe. In this work, we report the formation of a series of high mixing entropy BMGs based on multiple major elements, which have unique characteristics of excellent glass-forming ability and mechanical properties compared with conventional BMGs. The high mixing entropy BMGs based on multiple major elements might be of significance in scientific studies, potential applications, and providing a novel approach in search for new metallic glass-forming systems.

© 2011 Elsevier B.V. All rights reserved.

Since the discovery of the glassy  $\text{Au}_{75}\text{Si}_{25}$  alloy in 1960s, intensive efforts had been made in the development of metallic glasses due to their excellent properties such as high strength near the theoretical prediction, large elastic strain, and good corrosion and wear resistances compared with their crystalline counterparts [1–4]. Through composition design, bulk metallic glasses (BMGs) were developed with a relatively low critical cooling rate of  $1\text{--}100\text{ K s}^{-1}$  and have exceptional high glass-forming ability (GFA) [2–6]. In the last decade, a lot of multicomponent BMGs such as Fe-, Zr-, Ti-, Cu-, and rare earth based alloys has been fabricated [2–7]. The crucial factors for the BMG formation include the numbers and atomic size of the constituent elements as well as the mixing enthalpy between the main elements [4]. It is noted that the main design concept of these multi-component BMGs is based on a single element such as Zr, Mg, Cu and Fe. Generally, the strategy for developing BMGs is to select one element as a base and some other elements to match the base element for a good glass-forming ability [2,7], which limits the development of more metallic glass systems. To break through the traditional strategy of alloy design, some BMGs based on multiple major elements were developed such as  $\text{Zr}_{50}\text{Cu}_{50}$ -based BMGs and  $(\text{Ti}_{33}\text{Zr}_{33}\text{Hf}_{33})_{40}(\text{Ni}_{50}\text{Cu}_{50})_{50}\text{Al}_{10}$  in ribbon form by melt-spinning [8–11]. These BMGs are alloys with a combination of more than 2 major elements [8–11].

In this letter, we report the formation of a series of high mixing entropy BMGs based on multiple principal elements. The glass-forming ability, features and mechanical properties of the high mixing entropy alloys were studied. We show that the selection of the multiple major component elements with high mixing entropy is another effective route for design new glassy alloys.

According to the Boltzmann's hypothesis on the relationship between the entropy and system complexity, the change in configurational entropy during the formation of a solid solution from  $n$  elements with an equimolar ratio can be calculated from the following equation: [12]

$$\Delta S_{\text{conf}} = -k \ln w = -R \ln \frac{1}{n} = R \ln n, \quad (1)$$

where  $k$  is Boltzmann's constant,  $w$  is the number of ways of mixing, and  $R$  is the gas constant. The high mixing entropy promotes the tendency of simple crystal structure such as BCC and FCC, even amorphous structure in high mixing entropy alloys due to slow atomic diffusion, which can be explained by kinetic theory. Along this idea, we selected Li, Ca, Sr, Yb and Mg to increase the mixing entropy of the alloy. By melting mixtures of  $\text{Li}_{55}\text{Mg}_{45}$  master alloy, Ca (99.0%), Sr(99.0%), Zn(99.9%) and Yb (99.0%) elements using induction-melting method in a quartz tube under vacuum (better than  $3.0 \times 10^{-3}$  Pa) and subsequently casting into copper mold, three multi-component BMGs listed in Table 1 were obtained in cylindrical shape (50 mm in length) and in plate form with shiny metallic surfaces like Zr- and Cu-based BMGs. The structure of the as-cast alloys was identified by X-ray diffraction (XRD) using a MAC M03 diffractometer with Cu  $K_{\alpha}$  radiation. Thermal properties were investigated in a Mettler Toledo differential scanning calorimeter DSC822e with a heating rate of 10 K/min under a continuous argon flow. The values of glass transition temperatures ( $T_g$ ), onset temperatures of the crystallization event ( $T_c$ ) and liquidus temperature  $T_l$  were determined from the thermal analysis traces. Acoustic velocities through the alloys were obtained by ultrasonic measurement performed on MATEC 6600 ultrasonic system using a pulse-echo-overlap method with a carrier frequency of 10 MHz and a resolution of 0.5 ns. Compression tests at room temperature (RT) were performed on a series of BMGs with gage aspect ratio of 2:1 cut out of the as-cast 2 mm

\* Corresponding author.

E-mail address: [hybai@iphy.ac.cn](mailto:hybai@iphy.ac.cn) (H.Y. Bai).

**Table 1**  
The high mixing entropy BMGs based on multiple major elements and their thermodynamic parameters, elastic moduli, and the values of glass transition temperature,  $T_g$ , crystallization temperature  $T_x$  and liquidus temperature  $T_l$ .

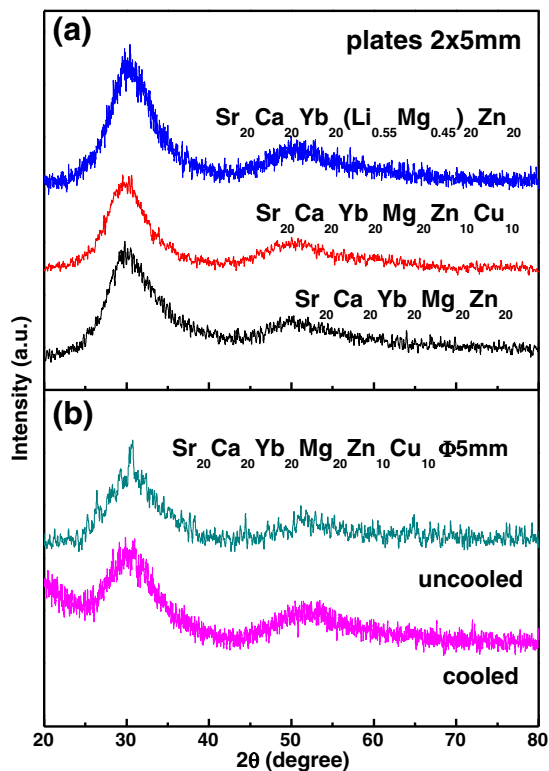
Alloy system	$\text{Sr}_{20}\text{Ca}_{20}\text{Yb}_{20}\text{Mg}_{20}\text{Zn}_{20}$	$\text{Sr}_{20}\text{Ca}_{20}\text{Yb}_{20}\text{Mg}_{20}\text{Zn}_{10}\text{Cu}_{10}$	$\text{Sr}_{20}\text{Ca}_{20}\text{Yb}_{20}(\text{Li}_{0.55}\text{Mg}_{0.45})_{20}\text{Zn}_{20}$
$T_g$ (K)	353	351	319
$T_x$ (K)	389	391	344
$T_l$ (K)	630	642	559
$\Delta T_x$ (K)	36	40	25
$T_{fg}$	0.56	0.55	0.57
$E$ (GPa)	22.8	24.3	16.1
$G$ (GPa)	8.89	9.47	6.28
$K$ (GPa)	17.5	18.6	12.4
$\nu$	0.283	0.282	0.283

rod at a strain rate of  $1 \times 10^{-4} \text{ s}^{-1}$  on Instron electromechanical testing system 3384.

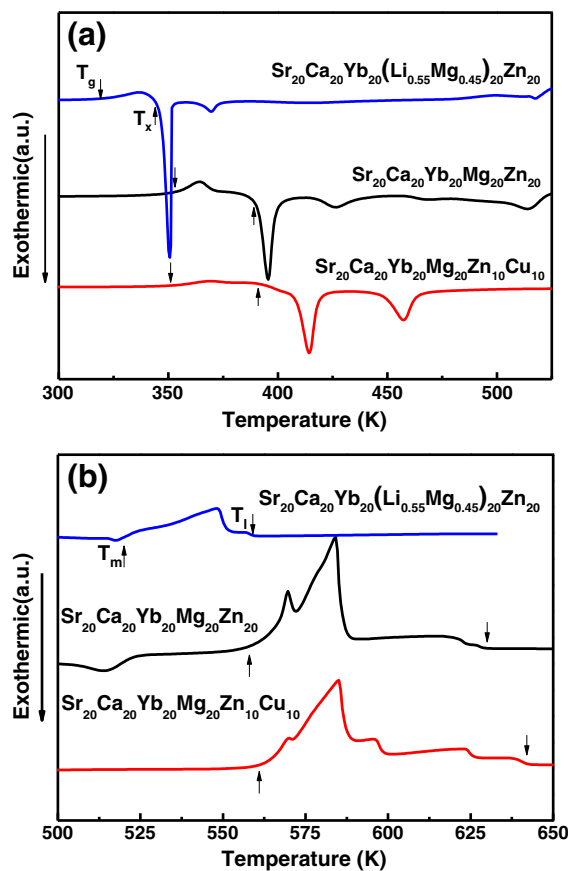
Fig. 1 shows the XRD patterns of as-cast samples of  $\text{Sr}_{20}\text{Ca}_{20}\text{Yb}_{20}\text{Mg}_{20}\text{Zn}_{20}$ ,  $\text{Sr}_{20}\text{Ca}_{20}\text{Yb}_{20}(\text{Li}_{0.55}\text{Mg}_{0.45})_{20}\text{Zn}_{20}$ , and  $\text{Sr}_{20}\text{Ca}_{20}\text{Yb}_{20}\text{Mg}_{20}\text{Zn}_{10}\text{Cu}_{10}$  alloys. For the alloys in plate form with the dimension of  $2 \times 5 \text{ mm}^2$ , the typical halo patterns for the amorphous phase were obtained and no diffraction peaks could be resolved within the resolution limit of the XRD as shown in Fig. 1a. Furthermore, the  $\text{Sr}_{20}\text{Ca}_{20}\text{Yb}_{20}\text{Mg}_{20}\text{Zn}_{10}\text{Cu}_{10}$  alloy in the rod with diameter up to 5 mm was cast in the copper mold, and the XRD pattern indicates that the alloy is not of full amorphous structure in this size. However, if the copper mold is cooled beforehand by liquid nitrogen, the fully glassy structure could be obtained in the rod with diameter up to 5 mm as shown in Fig. 1b. We note that a diameter of 2 mm high entropy  $\text{Er}_{20}\text{Tb}_{20}\text{Dy}_{20}\text{Ni}_{20}\text{Al}_{20}$  alloy with good GFA can also be easily cast into bulk glasses.

Fig. 2 shows the DSC curves of as-cast  $\text{Sr}_{20}\text{Ca}_{20}\text{Yb}_{20}(\text{Li}_{0.55}\text{Mg}_{0.45})_{20}\text{Zn}_{20}$ ,  $\text{Sr}_{20}\text{Ca}_{20}\text{Yb}_{20}\text{Mg}_{20}\text{Zn}_{10}\text{Cu}_{10}$ , and  $\text{Sr}_{20}\text{Ca}_{20}\text{Yb}_{20}\text{Mg}_{20}\text{Zn}_{20}$  samples taken from the fully glass plates. Each curve exhibits a pattern with an apparent endothermic event associate with glass transition and a

following multi-step crystallization process consisting of three visible exothermic peaks. The distinct glass transition and sharp crystallization events further confirm the fully amorphous structure of the BMGs. The  $T_g$ ,  $T_x$ , and the supercooled liquid region ( $\Delta T_x$ ) defined as  $\Delta T_x = T_x - T_g$  of the three metallic glass systems, are determined and summarized in Table 1. For  $\text{Sr}_{20}\text{Ca}_{20}\text{Yb}_{20}(\text{Li}_{0.55}\text{Mg}_{0.45})_{20}\text{Zn}_{20}$  and  $\text{Sr}_{20}\text{Ca}_{20}\text{Yb}_{20}\text{Mg}_{20}\text{Zn}_{10}\text{Cu}_{10}$ , which are obtained by substituting Li for 11% Mg and Cu for 10% Zn respectively, the crystallization processes are simpler compared with that of  $\text{Sr}_{20}\text{Ca}_{20}\text{Yb}_{20}\text{Mg}_{20}\text{Zn}_{20}$  as seen in Fig. 2a, which indicates that  $\text{Sr}_{20}\text{Ca}_{20}\text{Yb}_{20}(\text{Li}_{0.55}\text{Mg}_{0.45})_{20}\text{Zn}_{20}$  and  $\text{Sr}_{20}\text{Ca}_{20}\text{Yb}_{20}\text{Mg}_{20}\text{Zn}_{10}\text{Cu}_{10}$  have simple crystal structure after crystallization due to the effect of high mixing entropy. The  $\text{Sr}_{20}\text{Ca}_{20}\text{Yb}_{20}(\text{Li}_{0.55}\text{Mg}_{0.45})_{20}\text{Zn}_{20}$  also has much lower  $T_g$  and  $T_x$  which can be attributed to the substitution of Li with quite low elastic moduli and melting point [13]. The  $\Delta T_x$  value of  $\text{Sr}_{20}\text{Ca}_{20}\text{Yb}_{20}(\text{Li}_{0.55}\text{Mg}_{0.45})_{20}\text{Zn}_{20}$  is only 25 K and much smaller than that of  $\text{Sr}_{20}\text{Ca}_{20}\text{Yb}_{20}\text{Mg}_{20}\text{Zn}_{10}\text{Cu}_{10}$  and  $\text{Sr}_{20}\text{Ca}_{20}\text{Yb}_{20}\text{Mg}_{20}\text{Zn}_{20}$  indicating



**Fig. 1.** XRD patterns of cross-section of as-cast samples with different dimensions for (a)  $\text{Sr}_{20}\text{Ca}_{20}\text{Yb}_{20}(\text{Li}_{0.55}\text{Mg}_{0.45})_{20}\text{Zn}_{20}$ ,  $\text{Sr}_{20}\text{Ca}_{20}\text{Yb}_{20}\text{Mg}_{20}\text{Zn}_{10}\text{Cu}_{10}$ , and  $\text{Sr}_{20}\text{Ca}_{20}\text{Yb}_{20}\text{Mg}_{20}\text{Zn}_{20}$  alloys in plate form, respectively, (b)  $\text{Sr}_{20}\text{Ca}_{20}\text{Yb}_{20}\text{Mg}_{20}\text{Zn}_{10}\text{Cu}_{10}$  alloy in the rod with diameter up to 5 mm.



**Fig. 2.** The DSC curves of as-cast  $\text{Sr}_{20}\text{Ca}_{20}\text{Yb}_{20}(\text{Li}_{0.55}\text{Mg}_{0.45})_{20}\text{Zn}_{20}$ ,  $\text{Sr}_{20}\text{Ca}_{20}\text{Yb}_{20}\text{Mg}_{20}\text{Zn}_{10}\text{Cu}_{10}$  and  $\text{Sr}_{20}\text{Ca}_{20}\text{Yb}_{20}\text{Mg}_{20}\text{Zn}_{20}$  samples in the temperature range of (a) crystallization and (b) melting. (Heating rate is 10 K/min).

a relatively less stable glass [14], which is consistent with the phenomenon of the crystallization of the glass in 7 days.

To obtain the  $T_i$  value, DSC scan was extended to a high temperature until the melting of the alloys took place, as shown in Fig. 2b. From the endothermic signal of the melting, we can deduce that the multicomponent alloys are off-eutectic compositions. The reduced glass transition temperatures  $T_{rg}$  ( $T_{rg} = T_g/T_i$ ),  $T_g$  and  $T_i$  of these alloys are also listed in Table 1. The value of  $T_{rg}$  for these alloys is quite large compared with the existing BMG systems, which indicates strong GFA for these high mixing entropy alloys [15,16].

Above results show that a series of high mixing entropy BMGs based on multiple major elements can be obtained by conventional Cu mold cast method. The high mixing entropy BMGs based on multiple major elements might be a novel approach in the search for new metallic glass-forming alloy systems. Intensive efforts may be worth to be carried out to investigate high mixing entropy BMGs and to search more amorphous alloy systems with excellent GFA and unique physical properties.

Fig. 3 shows the compressive stress–strain curves of as-cast rods of  $\text{Sr}_{20}\text{Ca}_{20}\text{Yb}_{20}(\text{Li}_{0.55}\text{Mg}_{0.45})_{20}\text{Zn}_{20}$ ,  $\text{Sr}_{20}\text{Ca}_{20}\text{Yb}_{20}\text{Mg}_{20}\text{Zn}_{10}\text{Cu}_{10}$  and  $\text{Sr}_{20}\text{Ca}_{20}\text{Yb}_{20}\text{Mg}_{20}\text{Zn}_{20}$  alloys with 2 mm in diameter. For the  $\text{Sr}_{20}\text{Ca}_{20}\text{Yb}_{20}\text{Mg}_{20}\text{Zn}_{10}\text{Cu}_{10}$  and  $\text{Sr}_{20}\text{Ca}_{20}\text{Yb}_{20}\text{Mg}_{20}\text{Zn}_{20}$  alloys, their values of fracture strength are 423 MPa and 382 MPa, respectively. After elastic deformation, almost no plastic deformation occurred in the two BMGs. While for  $\text{Sr}_{20}\text{Ca}_{20}\text{Yb}_{20}(\text{Li}_{0.55}\text{Mg}_{0.45})_{20}\text{Zn}_{20}$  BMG, after elastic strain limit of ~2% (the yield strength  $\sigma_y$  is about 383 MPa), it remarkably displays stress overshoot as is often observed in homogeneous deformation in the supercooled liquid state, which is generally thought to be caused by the change in free volume during deformation. After the overshoot, the stress  $\sigma$  attains a steady state as shown in Fig. 3. Such exceptional deformability and flexibility observed in supercooled liquid state at room temperatures are due to the ultralow value of  $T_g$  for the  $\text{Sr}_{20}\text{Ca}_{20}\text{Yb}_{20}(\text{Li}_{0.55}\text{Mg}_{0.45})_{20}\text{Zn}_{20}$  BMG [17,18].

The elastic moduli were determined from acoustic velocities measurements and the results are listed in Table 1. The value of Poisson's ratio  $\nu$  for the three alloys is almost the same. The elastic moduli such as  $G$  and  $E$  are ultralow compared with that of other conventional BMGs [13]. The elastic constants ( $M$ ) of metallic glass can be estimated using equation  $M^{-1} = \sum f_i M_i^{-1}$ , where  $M_i$  and  $f_i$  denote elastic constant and atomic percentage of each constituent element, respectively [13]. Therefore, the substitution of Li for Mg which have very low elastic moduli makes the modulus of  $\text{Sr}_{20}\text{Ca}_{20}\text{Yb}_{20}(\text{Li}_{0.55}\text{Mg}_{0.45})_{20}\text{Zn}_{20}$  remarkably low, which causes the ultralow  $T_g$  [13]. According to shear cooperative model [19], the flow barrier energy  $W_{\text{STZ}}$  of shear transformation zones (STZs) in metallic glasses can be estimated by  $W_{\text{STZ}} \propto G V_m$  [20], where  $V_m$  is average molar volume. The BMGs with lower  $W_{\text{STZ}}$  generally have good ductility. Due to the ultra-

low  $G$  (6.3 GPa), the BMGs have much lower activation energy for STZ compared with that of other known BMGs, the activation of STZs is then much easier, which leads to the homogenous flow in the BMG. This is the case of applied stress induced glass transition at RT, which confirms the similarity and correlation between the plastic flow and the glass transition in metallic glasses [19,21,22]. On the other hand, the results indicate that the decrease of  $T_g$  or  $G$  by design is another route for the design of ductile metallic glasses.

The molding and imprinting previously reported for oxide glasses and conventional metallic glasses have to be performed at higher temperatures. For oxide glasses, for example,  $T_g > 1000$  K; and for Zr-, Fe-, Cu-based metallic glasses,  $T_g$  is above 500 K and even more. Because of the high  $T_g$ , molding of BMGs is often performed as part of the original quench, in a squeezing-casting or high-pressure casting process. In contrast, the  $\text{Ca}_{20}\text{Sr}_{20}\text{Yb}_{20}(\text{Li}_{0.55}\text{Mg}_{0.45})_{20}\text{Zn}_{20}$  BMG has relatively larger supercooled liquid region compared to conventional metallic glass ribbons and ultralow  $T_g$ , which makes the BMG show polymer-like thermoplastic formability near or even at room temperature. Fig. 4 shows the square array of BMG imprinted at room temperature, which indicates the super thermoplastic formability of the BMG. The BMG can be repeatedly compressed, stretched, bent, formed into complicated shapes even nano-imprinted patterns demonstrating the excellent thermoplastic processability as the conventional polymeric materials [23,24].

The metallic glass is one of the simplest glasses, and its microstructure units are composed of metallic atoms. It is close to a dense random packing of spheres without the complex intramolecular effect, rotational degree of freedom, or angle jump. The low  $T_g$  BMG offer a model system to study some fundamental issues in glassy physics. For example, due to the stable metallic supercooled liquids near RT, the BMG makes it possible to observe the intrinsic viscous behavior of the metallic glass around ambient temperature. It is widely recognized that the slow  $\beta$ -relaxations relate to mechanical properties, and BMG with ultralow  $T_g$  is readily for the measurement of the effect of slow  $\beta$ -relaxation on the properties of glass at RT, and promote the understanding of the slow  $\beta$ -relaxation. On the other hand, the homogeneous deformation is typically obtained and studied at high temperatures where relaxation dominates, and the effects of deformation are correspondingly difficult to detect in the final structure. This BMG system may provide an ideal case to investigate the true structural effects of shear events during homogeneous deformation and facilitate the experimental study of the deformation mechanism and structural evolution for metallic glasses.

In conclusions, high mixing entropy  $\text{Sr}_{20}\text{Ca}_{20}\text{Yb}_{20}(\text{Li}_{0.55}\text{Mg}_{0.45})_{20}\text{Zn}_{20}$ ,  $\text{Sr}_{20}\text{Ca}_{20}\text{Yb}_{20}\text{Mg}_{20}\text{Zn}_{10}\text{Cu}_{10}$ , and  $\text{Sr}_{20}\text{Ca}_{20}\text{Yb}_{20}\text{Mg}_{20}\text{Zn}_{20}$  BMGs with high glass-forming ability are obtained. These BMGs behave unique physical and mechanical properties, and could offer ideal model to

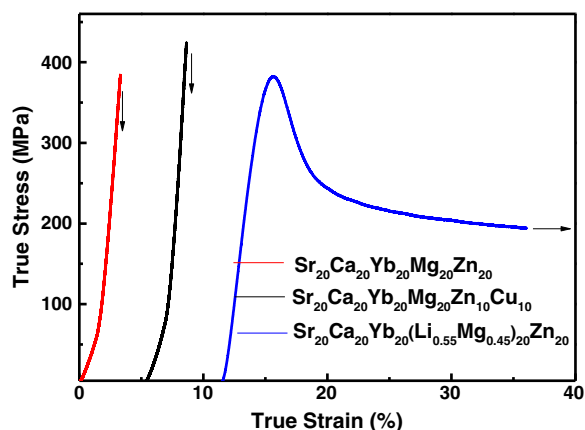


Fig. 3. The compressive stress–strain curves of as-cast rods for  $\text{Sr}_{20}\text{Ca}_{20}\text{Yb}_{20}(\text{Li}_{0.55}\text{Mg}_{0.45})_{20}\text{Zn}_{20}$ ,  $\text{Sr}_{20}\text{Ca}_{20}\text{Yb}_{20}\text{Mg}_{20}\text{Zn}_{10}\text{Cu}_{10}$  and  $\text{Sr}_{20}\text{Ca}_{20}\text{Yb}_{20}\text{Mg}_{20}\text{Zn}_{20}$  BMGs.

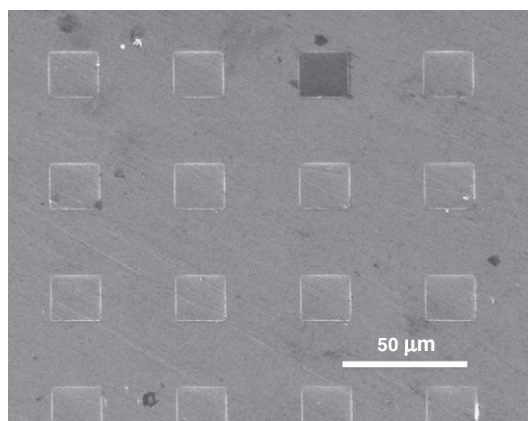


Fig. 4. Square array of the high entropy  $\text{Sr}_{20}\text{Ca}_{20}\text{Yb}_{20}(\text{Li}_{0.55}\text{Mg}_{0.45})_{20}\text{Zn}_{20}$  BMG imprinted in air condition at room temperature.

investigate some fundamental issues such as the glass transition and deformation mechanism in metallic glasses. The work provides a novel approach in the search for new metallic glass-forming systems with unique properties.

### Acknowledgments

Financial support from the NSF of China (50921091 and 50731008) and MOST973 of China (2007CB613904 and 2010CB731603) is greatly appreciated. Experimental aid of D.Q. Zhao is acknowledged.

### References

- [1] H.S. Chen, Rep. Prog. Phys. 43 (1980) 353.
- [2] A. Inoue, Acta Mater. 48 (2000) 279.
- [3] a) W.H. Wang, Prog. Mater. Sci. 52 (2007) 540;  
b) W.H. Wang, Adv. Mater. 21 (2009) 4524.
- [4] A.L. Greer, Nature 336 (1993) 303.
- [5] A. Peker, W.L. Johnson, Appl. Phys. Lett. 63 (1993) 2342.
- [6] a) Q. Luo, W.H. Wang, J. Non-Cryst. Solids 355 (2009) 759;  
b) S. Li, R.J. Wang, W.H. Wang, J. Non-Cryst. Solids 354 (2008) 1080.
- [7] Y. Li, S.J. Poon, J. Xu, D.H. Kim, J.F. Loeffler, MRS Bull. 32 (2007) 624.
- [8] J.W. Yeh, S.K. Chen, S.J. Lin, Adv. Eng. Mater. 6 (2004) 299.
- [9] B. Cantor, I.T.H. Chang, P. Knight, Sci. Eng. A 375–377 (2004) 213.
- [10] P. Yu, H.Y. Bai, W.H. Wang, J. Mater. Res. 21 (2006) 1674.
- [11] K.B. Kim, P.J. Warren, B. Cantor, J. Non-Cryst. Solids 317 (2003) 17.
- [12] R.A. Swalin, Thermodynamics of Solids, Wiley, New York, 1991.
- [13] W.H. Wang, J. Appl. Phys. 99 (2006) 093506.
- [14] A. Inoue, Mater. Trans. JIM 36 (1995) 866.
- [15] Z.P. Lu, Y. Li, J. Non-Cryst. Solids 270 (2000) 103.
- [16] F.Q. Guo, S.J. Poon, G.J. Shiflet, Scripta Mater. 43 (2000) 1089.
- [17] C.A. Schuh, T.C. Hufnagel, U. Ramamurty, Acta Mater. 55 (2007) 4067.
- [18] K. Zhao, H.Y. Bai, D.Q. Zhao, W.H. Wang, Appl. Phys. Lett. 98 (2011) 141913.
- [19] H.B. Yu, W.H. Wang, H.Y. Bai, Y. Wu, M.W. Chen, Phys. Rev. B 81 (2010) 220201.
- [20] W.L. Johnson, K. Samwer, Phys. Rev. Lett. 95 (2005) 195501.
- [21] Y.H. Liu, C.T. Liu, W.H. Wang, A. Inoue, M.W. Chen, Phys. Rev. Lett. 103 (2009) 065504.
- [22] H.B. Ke, P. Wen, D.Q. Zhao, W.H. Wang, Appl. Phys. Lett. 96 (2010) 251902.
- [23] B. Zhang, D.Q. Zhao, M.X. Pan, W.H. Wang, A.L. Greer, Phys. Rev. Lett. 94 (2005) 205502.
- [24] G. Kumar, H.X. Tang, J. Schroers, Nature 468 (2009) 457.